Pergamon

Int. J. Solids Structures Vol. 31, No. 3, pp. 291–302, 1994
Elsevier Science Ltd
Printed in Great Britain
0020–7683/94 $6.00 + .00

SCALING LAWS AND RENORMALIZATION GROUPS FOR STRENGTH AND TOUGHNESS OF DISORDERED MATERIALS†

ALBERTO CARPINTERI
Politecnico di Torino, Department of Structural Engineering, Corso Duca degli Abruzzi 24, 10129 Torino, Italy

(*Received* 28 *July* 1993)

Abstract—The abundant literature on tensile strength and fracture energy size effects as well as the newly-introduced fractal and renormalization group theories would appear to indicate the need for a dramatic change in our conceptual framework, if we want to consider and measure material constants in Strength of Materials as well as in Fracture Mechanics. For disordered materials, such as for example concrete and rocks, the renormalized tensile strength is given by a force acting on a surface having a fractal dimension lower than 2, just as the renormalized fracture energy is represented by a dissipation over a surface with a dimension higher than 2. In the case of tensile strength, the dimensional decrement represents self-similar weakening of the reacting cross section or ligament, due to pores, voids, defects, cracks, aggregates, inclusions, etc. Likewise, in the case of fracture energy, the dimensional increment represents self-similar tortuosity of the fracture surface, due to aggregates and inclusions, as well as self-similar microcrack overlapping and distribution also in the direction orthogonal to that of the forming macrocrack. It can be demonstrated that the sum of the dimensional decrement (for material ligament) and the dimensional increment (for fracture surface) must be lower than unity.

INTRODUCTION

Renormalization group theories have been shown to be necessary in many branches of physics, whenever many length or energy scales are present in the problem to be solved. These problems include quantum field theory, statistical mechanics, turbulence, blasting (Wilson, 1971, 1979; Barenblatt, 1979; Herrmann and Roux, 1990), etc.

Several physical phenomena can be analysed through continuum mechanics, whenever only one length or energy scale is relevant, namely the macroscopic scale. On the other hand, it is generally true that, where a critical phenomenon (e.g., material failure) is imminent, also other length or energy scales become relevant together with the macroscopic one: they represent those microscopic or mesoscopic phenomena that are interacting and concurring to produce the macroscopic phenomenon. Continuum mechanics has been the basis for structural mechanics for more than a century. Only recently has it emerged that damage, strain localization, and fracture phenomena are not always interpretable in the framework of continuum mechanics. In particular, the scale effects on strength and toughness have not found satisfactory explanations (Carpinteri, 1986). The reason for this has to be sought in the fact that the micromechanical damage phenomena, and thus the inherent disorder of the material, have been disregarded. A dramatic dichotomy is still present between, on the one hand, structural engineers, who pay close attention to macroscopic phenomena and whose models present an excessive regularity, and, on the other, material scientists, who devote greater attention to microscopic phenomena and whose models present an excessively local character.

The present paper represents an attempt to break down these barriers by adopting approaches that are completely new for solid mechanics, i.e., fractal geometry (Mandelbrot, 1982; Falconer, 1990) and renormalization group theory (Wilson, 1971, 1979; Barenblatt, 1979; Herrmann and Roux, 1990). This is the only way to provide a rational and consistent explanation of the size scale effects on tensile strength and fracture energy of disordered materials. For size scale tending to zero, tensile strength tends to infinity, whereas fracture energy tends to zero. The renormalized counterparts of such properties are instead constant

† Transmitted by Professor B. L. Karihaloo (Board of Editors).

and tend to render their physical roles coincident when a condition of extreme disorder is achieved at small size scales.

FRACTAL NATURE OF MATERIAL LIGAMENT AND SIZE EFFECTS ON NOMINAL TENSILE STRENGTH

It is well-known that the nominal tensile strength of many materials undergoes very clear size effects. The usual trend is that of a strength decrease with size, and this is more evident for disordered (i.e. macroscopically heterogeneous and/or damaged) materials. Griffith (1921) explained the strength size effect in the case of glass filaments, assuming the existence of inherent microcracks of a size proportional to the filament cross-sectional diameter. Some years later Weibull (1939) gave a purely statistical explanation to the same phenomenon according to the weakest-link-in-a-chain concept. Only recently have the two views been harmonized, enriching the empirical approach of Weibull with the phenomenological assumption of Griffith (Freudenthal, 1968; Jayatilaka, 1979; Carpinteri, 1989a). A statistical size distribution of self-similarity may be defined (Carpinteri, 1986, 1989a) for which the most dangerous defect proves to be of a size proportional to the structural size. This corresponds to materials presenting a considerable dispersion in the statistical microcrack size distributions (disordered materials). In this case, the power of the LEFM stress singularity, 1/2, turns out to be the slope of the strength vs size decrease in a bilogarithmic diagram. When the statistical dispersion is relatively low (ordered materials) the slope is less than 1/2 and tends to zero for regular distributions (perfectly ordered materials).

Although the above-described view contains the fractal concept of self-similarity, this is circumscribed only to the defect of maximum size, whereas the disordered nature of the material microstructure is completely disregarded. The real nature of the material will be herein described using a more complex fractal model, where the property of self-similarity is extended to the whole defect population. This model represents a more realistic picture of reality and is consistent with the fractal explanation of the fracture energy size effect, which will be proposed in the next section. On the other hand, as will be shown, slope values higher than 1/2 would represent, with both models, a degree of disorder that is so high as to be usually absent in real materials.

Let us assume that the reacting section or ligament of a disordered material at peak stress could be represented as a fractal space of dimension $\alpha = 2-d_\sigma$, with $1 < \alpha \leqslant 2$ and, therefore, $0 \leqslant d_\sigma < 1$. The dimensional decrement d_σ may be due to the presence of cracks and voids and hence, generally, to a cross-sectional weakening. Let us consider two bodies, geometrically similar and made up of the same disordered material [Fig. 1(a)]. If the ratio of geometrical similitude is equal to b and the *renormalized tensile strength* σ_u^* is assumed to be a material constant and to have the physical dimensions [force] $\times$ [length]$^{-(2-d_\sigma)}$, we have:

$$\sigma_u^* = \frac{F_1}{1^{2-d_\sigma}} = \frac{F_2}{b^{2-d_\sigma}}, \tag{1}$$

F_1 and F_2 being the ultimate tensile forces acting on the two bodies respectively.

On the other hand, the apparent nominal tensile strengths are respectively:

$$\sigma_u^{(1)} = \frac{F_1}{1^2}, \tag{2a}$$

$$\sigma_u^{(2)} = \frac{F_2}{b^2}, \tag{2b}$$

where the latter, according to eqn (1), becomes:

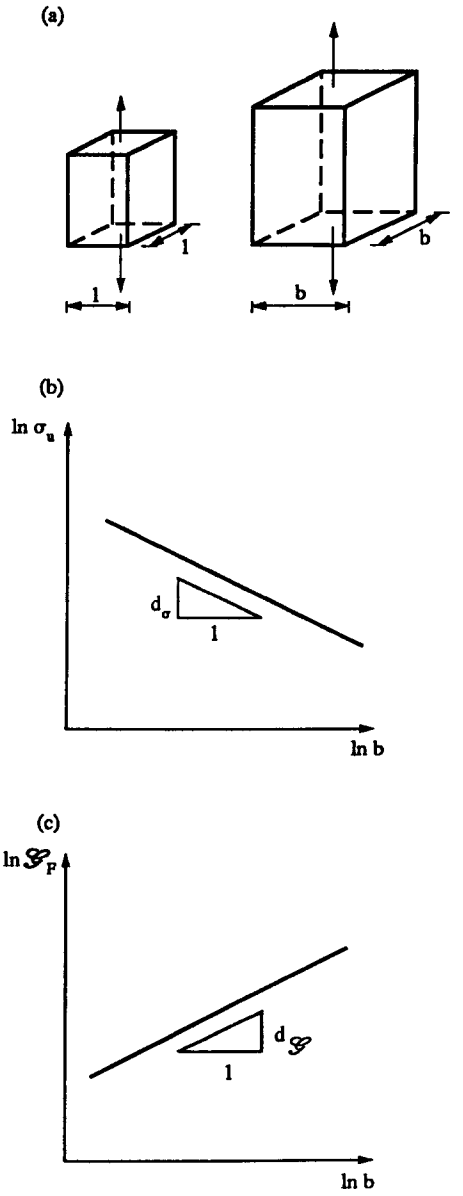

Fig. 1. (a) Size-scaled bodies; (b) correlated size-scale effects on tensile strength; and (c) fracture energy.

$$\sigma_u^{(2)} = \sigma_u^{(1)} b^{-d_\sigma}. \tag{3}$$

We can write the relationship between nominal strengths related to different sizes in logarithmic form:

$$\ln \sigma_u = \ln \sigma_u(1) - d_\sigma \ln b. \tag{4}$$

Equation (4) represents a straight line with slope $-d_\sigma$ in the $\ln \sigma_u$ vs $\ln b$ plane [Fig. 1(b)].

An alternative way to explain the decrease of the nominal tensile strength with specimen size is that of considering a sequence of scales of observation. If the total force F transmitted to the specimen is invariant with respect to the scale of observation, we have:

$$F = \sigma_1 A_1 = \sigma_2 A_2 = \cdots = \sigma_{n-1} A_{n-1} = \sigma_n A_n = \sigma_{n+1} A_{n+1} = \cdots = \sigma_\infty A_\infty, \tag{5}$$

where the first scale of observation could be the macroscopic one, with $\sigma_1 A_1 = \sigma_u A$, A being the cross-sectional area, and the asymptotic scale of observation could be the microscopic one, with $\sigma_\infty A_\infty = \sigma_u^* A^*$, A^* being the measure of the fractal set representing the damaged ligament.

From the equality between the extreme members of eqn (5) we get:

$$\sigma_u = \sigma_u^* \left(\frac{A^*}{A}\right), \tag{6}$$

and therefore:

$$\sigma_u = \sigma_u^* \left(\frac{b^{2-d_\sigma}}{b^2}\right) \tag{7}$$

with b equal to the characteristic dimension of the cross section. From eqn (7) we can get a generalization of eqn (4):

$$\ln \sigma_u = \ln \sigma_u^* - d_\sigma \ln b. \tag{8}$$

Renormalization group relations analogous to eqn (8) have been proposed by Wilson (1971, 1979) in quantum field theory and statistical mechanics, as well as by Barenblatt (1979) in the intermediate asymptotics description of turbulence and blasting.

Confirmation of eqn (4) has been provided by several previous investigations, carried out on different metallic and cementitious materials and with different specimen geometries. These results are summarized in Carpinteri (1989a). The same trends have been found also in two recent experimental programmes aimed at evaluating the true tensile properties of concrete. A completely new testing apparatus made up of three orthogonally disposed actuators, was utilized at the Politecnico di Torino so that it was possible to perform a true direct tensile experiment on concrete, whereas usually tension and bending are both present. As may be seen from Fig. 2(a), the slope of the strength decrease proved to be equal to

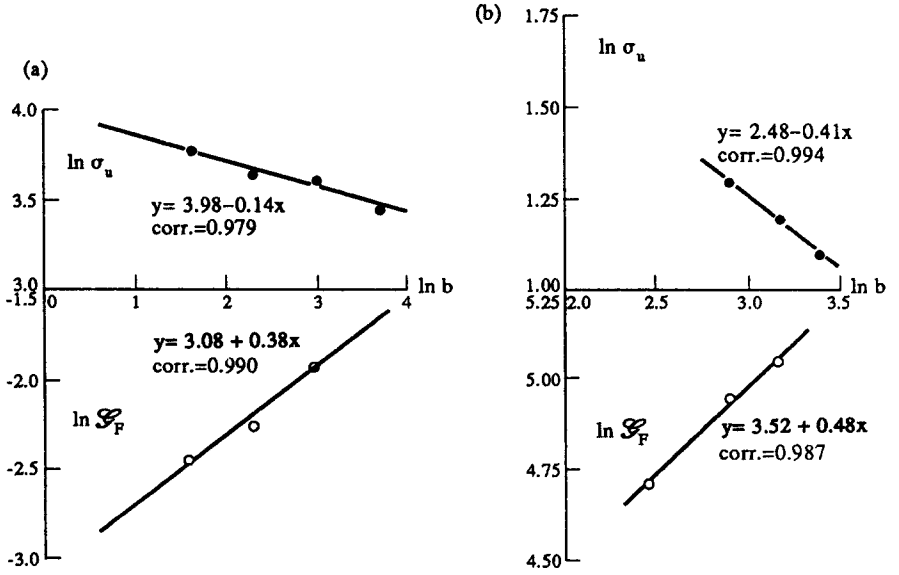

Fig. 2. Experimental results obtained by the author (a) at the Politecnico di Torino and (b) in collaboration with ENEL-CRIS-Milano and ISMES-Bergamo.

0.14, thus revealing a material ligament of dimension 1.86, i.e. a fractal set which is very close to a two-dimensional surface. It may be noted that the specimen sizes explored in this investigation ranged over four values of the width: 5, 10, 20 and 40 cm. The fractal nature of the material ligament emerges very clearly at such scales. On the other hand, the property of self-similarity is very likely to vanish or change at higher or lower scales, owing to the limited character of the granulometric curve.

A higher slope of strength decrease was obtained in an experimental research study performed at ISMES-Bergamo, using pre-notched concrete cylinders of diameter 12, 18, 24 and 30 cm, respectively [Fig. 2(b)]. The exponent 0.41 is closer to the LEFM limit 0.5, which is valid for disordered materials (high statistical dispersion), and at the same time implies a very weak fractal ligament of dimension 1.59 at peak stress.

FRACTAL NATURE OF FRACTURE SURFACE AND SIZE EFFECTS ON FICTITIOUS FRACTURE ENERGY

It is well-known how the fracture surfaces of metals (Mandelbrot *et al.*, 1984) and concrete (Saouma *et al.*, 1990) present a fractal nature with a roughness producing a dimensional increment with respect to the number 2. Even in this case we can detect an evident mechanical consequence, considering the size effects on fracture energy $\mathcal{G}_F$. Since Hillerborg's proposal for a concrete fracture test was published as RILEM Recommendation (1985), several researchers have measured a fracture energy $\mathcal{G}_F$ which increases with the specimen sizes and, more specifically, with the size of the uncracked ligament. Such a trend has been systematically found, and in each case the authors of the papers describing these experiments have tried to provide various empirical or phenomenological explanations, without, however, endeavouring to interpret their findings in a larger conceptual framework. On the other hand, if we wish to understand the experimental observations, it is necessary to abandon the classical thermodynamic concept of surface energy of an ideal solid, and to assume the energy dissipation to be occurring in a fractal space of dimension $\alpha = 2 + d_{\mathcal{G}}$, with $2 \leqslant \alpha < 3$ and, therefore, $0 \leqslant d_{\mathcal{G}} < 1$. This represents an attenuation of fracture localization due to material heterogeneity and multiple cracking.

Let us consider two bodies, geometrically similar and made up of the same disordered material [Fig. 1(a)]. If the ratio of geometrical similitude is equal to b and the *renormalized fracture energy* $\mathcal{G}_F^*$ is assumed to be a material constant and to have the physical dimensions [force] × [length]$^{-(1+d_{\mathcal{G}})}$, we obtain:

$$\mathcal{G}_F^* = \frac{W_1}{1^{2+d_{\mathcal{G}}}} = \frac{W_2}{b^{2+d_{\mathcal{G}}}} \tag{9}$$

W_1 and W_2 being the energies dissipated in the two bodies respectively.

On the other hand, the apparent fictitious fracture energies are respectively:

$$\mathcal{G}_F^{(1)} = \frac{W_1}{1^2}, \tag{10a}$$

$$\mathcal{G}_F^{(2)} = \frac{W_2}{b^2}, \tag{10b}$$

where the latter, according to eqn (9), becomes:

$$\mathcal{G}_F^{(2)} = \mathcal{G}_F^{(1)} b^{d_{\mathcal{G}}}. \tag{11}$$

We can write the relationship between fracture energies related to different sizes in logarithmic form:

$$\ln \mathcal{G}_F = \ln \mathcal{G}_F(1) + d_{\mathcal{G}} \ln b. \tag{12}$$

Equation (12) represents a straight line with slope $d_{\mathcal{G}}$ in the $\ln \mathcal{G}_F$ vs $\ln b$ plane [Fig. 1(c)].

An alternative way of explaining the increase of the fracture energy with specimen size is that of considering a sequence of scales of observation. If the total energy W dissipated by fracture is invariant with respect to the scale of observation, we have:

$$W = \mathcal{G}_1 A_1 = \mathcal{G}_2 A_2 = \ldots = \mathcal{G}_{n-1} A_{n-1} = \mathcal{G}_n A_n = \mathcal{G}_{n+1} A_{n+1} = \ldots = \mathcal{G}_\infty A_\infty, \tag{13}$$

where the first scale of observation could be the macroscopic one, with $\mathcal{G}_1 A_1 = \mathcal{G}_F A$, A being the cross-sectional area, and the asymptotic scale of observation could be the microscopic one, with $\mathcal{G}_\infty A_\infty = \mathcal{G}_F^* A^*$, A^* being the measure of the fractal set representing the irregular fracture surface.

From the equality between the extreme members of eqn (13) we get:

$$\mathcal{G}_F = \mathcal{G}_F^* \left(\frac{A^*}{A} \right), \tag{14}$$

and therefore

$$\mathcal{G}_F = \mathcal{G}_F^* \left(\frac{b^{2+d_{\mathcal{G}}}}{b^2} \right), \tag{15}$$

with b equal to the characteristic dimension of the cross section. From eqn (15) we can get a generalization of eqn (12)

$$\ln \mathcal{G}_F = \ln \mathcal{G}_F^* + d_{\mathcal{G}} \ln b. \tag{16}$$

On the other hand, if the pioneering work of Griffith (1921) is revisited considering a fractal crack of projected length $2a$, the fundamental relation of energy balance becomes:

$$\frac{\sigma^2}{E} \mathrm{d}(\pi a^2) = 2 \mathcal{G}_F^* \mathrm{d}(a^{1+d_{\mathcal{G}}}), \tag{17}$$

and therefore

$$\pi \frac{\sigma^2}{E} a \, \mathrm{d}a = \mathcal{G}_F^* (1 + d_{\mathcal{G}}) a^{d_{\mathcal{G}}} \, \mathrm{d}a. \tag{18}$$

From eqn (18) we get:

$$\sigma^2 \pi a^{1-d_{\mathcal{G}}} = (1 + d_{\mathcal{G}}) \mathcal{G}_F^* E, \tag{19}$$

which represents the renormalized critical condition:

$$(K_I^*)^2 = (K_{IC}^*)^2. \tag{20}$$

The generalized stress-intensity factor K_I^* presents the following physical dimensions: $[F]\,[L]-(3+d_{\mathcal{G}})/2$. When $d_{\mathcal{G}} = 0$, we find again the classical relations of Griffith and Irwin. When $d_{\mathcal{G}} = 1$, as a limit case, we find that the stress singularity vanishes and K_I^* assumes the physical dimensions of stress. Similar dimensional transitions have been analysed by the writer for strain-hardening materials in the presence of cracks (Carpinteri, 1983) and for linear elastic materials in the presence of re-entrant corners (Carpinteri, 1987).

The same trends of eqn (12) have been found in recent experimental studies. Tensile testing performed at the Politecnico di Torino has provided a plot slope equal to 0.38 [Fig. 2(a)], which allows a constant (universal) energy parameter to be obtained in the case where the dissipation is considered as occurring in a damaged space of dimension 2.38. Tensile testing at ISMES-Bergamo [Fig. 2(b)] has provided a plot slope very close to the LEFM singularity 1/2, namely 0.48, and thus a fractal dimension 2.48, which implies a very disordered material. It is interesting to note that the range of self-similarity does not extend to the largest size for $\mathscr{G}_F$, just as it does not extend to the smallest size for σ_u. So the ranges of self-similarity for fracture energy and tensile strength do not necessarily coincide.

CONDITIONS OF EXTREME DISORDER

Let us consider a set of similar bodies with a multitude of imperfections (cracks, voids, etc.) of a given size distribution. If the imperfections with the most dangerous shape produce a stress-singularity $r^{-\lambda}(0 < \lambda \leqslant \frac{1}{2})$ and present a probability density $p(a)$ of size distribution [Fig. 3(a, b)], and if $p(a)$ is such that the maximum size $a_{\max}$ is proportional to the linear scale b, then the strength size effect will be represented by a linear ln σ_u vs ln b diagram with slope $-\lambda$. The above hypothesis is very restrictive and is valid only when the size distribution $p(a)$ presents particular properties.

If ρ is the density of imperfections (number of imperfections per unit volume), the maximum size $a_{\max}$ can be defined as follows:

$$\rho b^3 p(a_{\max}) \Delta a \frac{1}{4\pi^2} \Delta\varphi \, \Delta\vartheta = 1, \tag{21a}$$

φ and ϑ being the longitude and the latitude of the defect orientation. If a geometrically

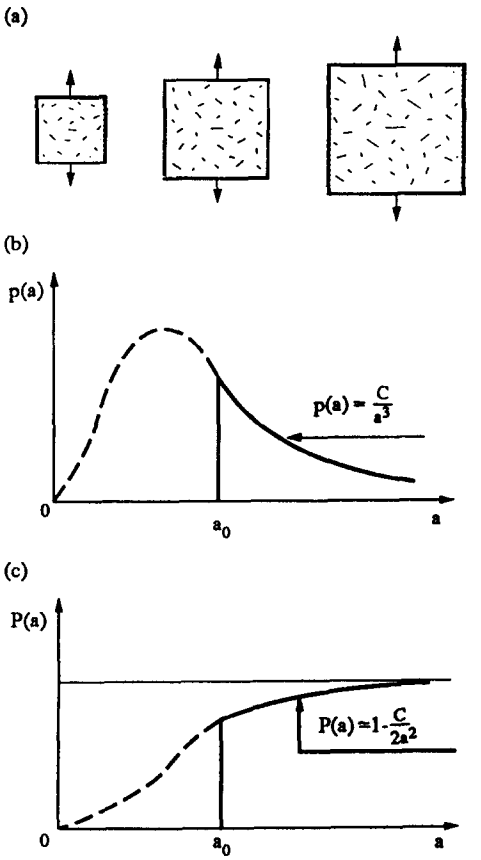

Fig. 3. (a) Geometrically similar bodies with many random defects; (b) defect size distribution of self-similarity and (c) cumulative distribution of self-similarity.

similar body of characteristic size kb is considered and the above hypothesis is assumed [Fig. 3(a)], we can write:

$$\rho(kb)^3 p(ka_{\max})\Delta a \frac{1}{4\pi^2}\Delta\varphi\,\Delta\vartheta = 1. \tag{21b}$$

Since $a_{\max}$ is a function of ρ and b, besides the ranges Δa, $\Delta\varphi$, $\Delta\vartheta$ of defect size, longitude, and latitude, respectively, it follows that eqns (21) must be valid for any defect size a. Therefore it follows that:

$$p(a) = k^3 p(ka), \quad \forall a \gg \bar{a}, \quad \forall k \in R^+, \tag{22}$$

and then function p assumes the form [Fig. 3(b)]

$$p(a) = \frac{C}{a^3}, \quad \forall a \gg \bar{a}, \tag{23}$$

where C is a constant with the physical dimension of a length and $\bar{a}$ is the average defect size. Equation (23) will be referred to as the *defect size distribution of self-similarity*. The related cumulative distribution function P is:

$$P(a) = \int_o^a p(x)\,dx = \int_o^{a_o} p(x)\,dx + \int_{a_o}^a \frac{C}{x^3}\,dx, \tag{24}$$

where $a_o \gg \bar{a}$ is the value beyond which the decreasing branch of function p can be approximated by eqn (23). Carrying out the integrations in eqn (24), we obtain:

$$P(a) = P_o + \left[-\frac{C}{2x^2}\right]_{a_o}^a = P_o + \frac{C}{2a_o^2} - \frac{C}{2a^2}. \tag{25}$$

Since for $a \to \infty$ the cumulative distribution $P(a) \to 1$

$$P_o + \frac{C}{2a_o^2} = 1 \tag{26}$$

and then [Fig. 3(c)]

$$P(a) = 1 - \frac{C}{2a^2} \tag{27}$$

with

$$C = 2(1 - P_o)a_o^2. \tag{28}$$

Generally speaking, when the condition of self-similarity is not satisfied, the cumulative distribution function P will have the following form:

$$P(a) = 1 - \frac{C}{Na^N}, \quad \text{for } a > a_o, \tag{29}$$

with

$$C = N(1-P_o)a_o^N, \tag{30}$$

where $N(1 < N < \infty)$ is an exponent measuring the degree of disorder. In this case, the strength size effect can be represented by a linear $\ln \sigma_u$ vs $\ln b$ diagram with slope $-\lambda_N$

$$\lambda_N = \frac{\lambda}{(N-1)^\zeta} \tag{31}$$

where the exponent ζ depends on the secondary features of the material (e.g. density of defects, size distribution of the less dangerous defects, etc.). The probability density of size distribution in the general case—see eqn (29)—is:

$$p(a) = \frac{dP}{da} = \frac{C}{a^{N+1}} \quad \text{for } a > a_o, \tag{32}$$

which becomes eqn (23) when $N = 2$.

Equation (31) shows that the size effect vanishes when $\lambda = 0$ (e.g. spherical pores) and/or when $N \to \infty$ (nearly constant defect size). On the other hand, the size effect becomes enormous when $N \to 1$ (very large dispersion in the defect size distribution).

Let us assume now that the defect size distribution is not that of self-similarity but one with a larger dispersion $(1 < N < 2)$. The maximum defect size a_{max} can be defined as in eqn (21a), whereas the maximum defect size for a geometrically similar body of characteristic size kb $(k > 1)$ will be given by a power law of the form:

$$a_{max}(k) = k^\beta a_{max}(1), \tag{33}$$

with $\beta > 1$.

Thus, eqn (21b) can be replaced by the following:

$$\rho(kb)^3 p(k^\beta a_{max}) \Delta a \frac{1}{4\pi^2} \Delta\varphi \, \Delta\vartheta = 1. \tag{34}$$

Equating eqn (21a) and eqn (34), and eliminating the subscript max, we obtain:

$$p(a) = k^3 p(k^\beta a), \tag{35}$$

and then, introducing eqn (32), we determine the exponent β as a function of N:

$$\beta = \frac{3}{N+1}. \tag{36}$$

It is not difficult to verify that, in the previous assumption and for sufficiently large sizes, the maximum defect proves to be larger than the body itself. In fact, eqns (33) and (36) give:

$$a_{max}(k) = k^{3/(N+1)} a_{max}(1), \tag{37}$$

which is a nonlinear function of k, whereas the characteristic size of the body increases linearly with k:

$$b(k) = kb = k\frac{a_{max}(1)}{\xi}. \tag{38}$$

The maximum defect is larger than the body itself:

$$a_{\max}(k) \geqslant b(k), \tag{39}$$

for

$$k \geqslant \xi^{(N-2)/(N+1)} > 1. \tag{40}$$

It is possible therefore to conclude that the defect size distribution of self-similarity is that corresponding to the maximum disorder.

From eqn (31) it is now possible to deduce the maximum slope of the strength decrease diagram. This is provided by three concurrent conditions:

(1) linear elastic material;
(2) Griffith cracks ($\lambda = 1/2$);
(3) maximum disorder ($N = 2$, i.e., self-similarity).

The slope 1/2 appears to be a theoretical upper bound, which is never exceeded in the experimental results reported in the relevant literature.

On the other hand, the zero slope (horizontal line) is the theoretical lower bound, which is given by even just one of the following three conditions:

(1) elastic-perfectly plastic material;
(2) pores not producing stress-singularity ($\lambda = 0$);
(3) maximum order ($N \to \infty$, i.e., Dirac-δ distribution).

CORRELATED RENORMALIZATION FOR STRENGTH AND TOUGHNESS

As regards the dimensional decrement d_σ, corresponding to the slope λ_N defined in eqn (31), as well as the dimensional increment $d_{\mathcal{G}}$, previously defined for the fracture energy, experimentally they both appear always comprised in the interval $[0, \frac{1}{2}]$. The dimensional decrement d_σ tends to the LEFM limit $\frac{1}{2}$ only for extremely brittle and disordered materials, as also does the dimensional increment $d_{\mathcal{G}}$. The explanation for the latter bound could arise for Dimensional Analysis reasons. A generalization of the *brittleness number* defined by the writer (Carpinteri, 1982, 1985, 1989b) could in fact be the following:

$$s_E^* = \frac{\mathcal{G}_F^*}{\sigma_u^* b^{(1-d_\sigma-d_{\mathcal{G}})}}. \tag{41}$$

If we postulate that the reversal of the physical roles of toughness and strength is absurd, the exponent of the characteristic linear size b must be positive:

$$d_\sigma + d_{\mathcal{G}} < 1. \tag{42}$$

The sum of the dimensional decrement (for material ligament) and the dimensional increment (for fracture surface) must therefore be lower than unity. On the other hand, when for very disordered materials we have $d_\sigma \simeq \frac{1}{2}$, the upper bound of eqn (42) becomes $d_{\mathcal{G}} \lesssim \frac{1}{2}$.

The above fractal interpretations could be regarded by some as purely mathematical abstractions, if not indeed distortions of reality. The truth is that both classical geometrical domains and fractal geometry loci are idealizations of reality. The question that should be answered is the following: which model is closer to a real fracture trajectory in a concrete specimen, a straight line or the von Koch curve? Of course the latter, even though the fractal nature of the fracture trajectory is random and valid only in a limited scale range. This means that, for size scales tending to infinity, or, in other words, for very large specimens, tensile strength σ_u and fracture energy $\mathcal{G}_F$ may appear constant by varying the specimen size, whereas, for size scales where random self-similarity holds, the so-called "universal properties" of the system (σ_u^*, $\mathcal{G}_F^*$) are constant, although they are represented by physical quantities with unusual dimensions. The last result represents the target of the so-called

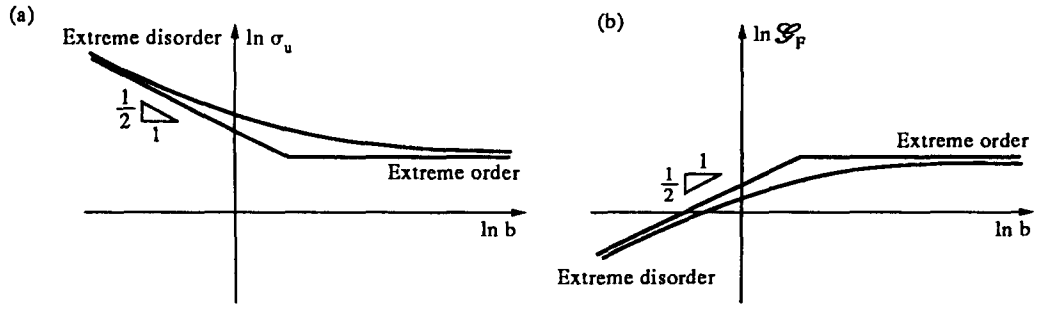

Fig. 4. (a) Multifractal scaling laws for tensile strength and (b) fracture energy. Bilogarithmic diagrams.

"renormalization" procedure (Wilson, 1971, 1979), i.e. the determination of physical quantities that are invariant under a change of length scale.

In physical reality, both material ligaments at peak stress and fracture surfaces after rupture can be considered as multifractals (Mandelbrot, 1982; Falconer, 1990), of dimension 1.5 and 2.5, respectively, at small scales, and dimension 2 at large scales. This means that, at large scales, the disorder is not visible, the size of the heterogeneities being limited. A transition from extreme disorder (slope 1/2) to extreme order (zero slope) may therefore be evidenced in both diagrams, namely ln σ_u vs ln b and ln $\mathcal{G}_F$ versus ln b (Fig. 4). Probably, for even smaller scales, a chaotic disorder could prevail over the maximum fractal disorder with slope 1/2.

The asymptotic trends of tensile strength and fracture energy can be described also in the corresponding proportional diagrams as in Fig. 5. For size scale tending to zero, tensile strength tends to infinity, whereas fracture energy tends to zero. Renormalization group theory, already applied in other branches of science, is able to provide a definitive and correlated explanation of the size effects on strength and toughness. We should recall the first attempt by Griffith (1921) to give some rational explanation to the strength increase by decreasing the cross-sectional area of glass filaments [Fig. 6(a)]. At the same time, Dimensional Analysis can provide us with some pointers to explaining the toughness decrease by decreasing specimen size, when stress-intensification does not develop at the crack tip (Carpinteri, 1982) [Fig. 6(b)]. In both cases the experimentalist presumes that he is measuring a material property, even though another critical phenomenon, and one not related to the same property, is occurring. In either case he ignores one of the two parameters—K_{IC} or σ_u—along with the related failure mechanism. The explanations provided by Dimensional Analysis are relatively simplistic, since σ_u and $\mathcal{G}_F$ are considered as material constants. In the real physical world, not only do σ_u and $\mathcal{G}_F$ not appear to be constant as the size scale varies, but also the renormalized counterparts of these two parameters tend

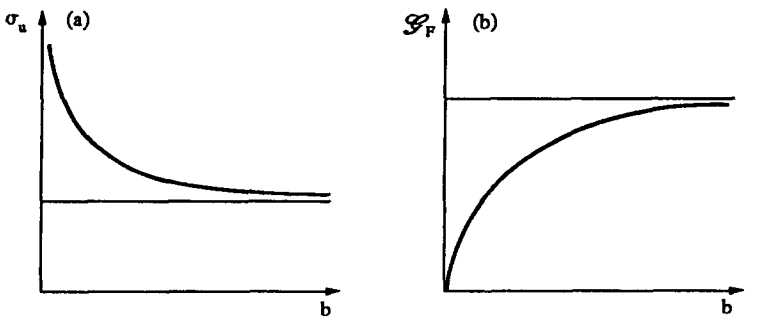

Fig. 5. (a) Multifractal scaling laws for tensile strength and (b) fracture energy. Proportional diagrams.

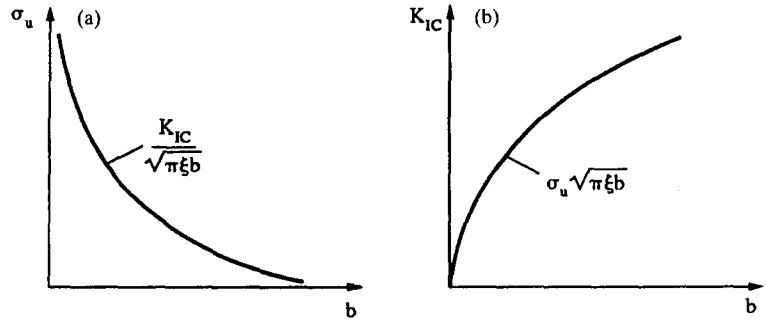

Fig. 6. Classical scaling laws provided by Dimensional Analysis. (a) Tensile strength variation according to Griffith and (b) fracture toughness variation for totally notch-insensitive specimens.

to render their physical roles coincident for very disordered materials or, in any case, at very small size scales.

Acknowledgements—The present research was carried out with the financial support of the Ministry for the University and for Scientific and Technological Research (MURST) and the National Research Council (CNR).

REFERENCES

Barenblatt, G. I. (1979). *Similarity, Self-Similarity and Intermediate Asymptotics*. Consultants Bureau, New York.

Carpinteri, A. (1982). Notch sensitivity in fracture testing of aggregative materials. *Engng Fract. Mech.* **16,** 467–481.

Carpinteri, A. (1983). Plastic flow collapse vs separation collapse (fracture) in elastic–plastic strain-hardening structures. *Mater. Struct.* **16,** 85–96.

Carpinteri, A. (1985). Interpretation of the Griffith instability as a bifurcation of the global equilibrium. In *Applications of Fracture Mechanics to Cementitious Composites* (Edited by S. P. Shah), pp. 287–316. Martinus Nijhoff Publishers, Dordrecht.

Carpinteri, A. (1986). *Mechanical Damage and Crack Growth in Concrete: Plastic Collapse to Brittle Fracture*. Martinus Nijhoff Publishers, Dordrecht.

Carpinteri, A. (1987). Stress-singularity and generalized fracture toughness at the vertex of re-entrant corners. *Engng Fract. Mech.* **26,** 143–155.

Carpinteri, A. (1989a). Decrease of apparent tensile and bending strength with specimen size: two different explanations based on fracture mechanics. *Int. J. Solids Structures* **25,** 407–429.

Carpinteri, A. (1989b). Cusp catastrophe interpretation of fracture instability. *J. Mech. Phys. Solids* **37,** 567–582.

Falconer, K. (1990). *Fractal Geometry: Mathematical Foundations and Applications*. Wiley, Chichester.

Freudenthal, A. M. (1968). Statistical approach to brittle fracture. In *Fracture* (Edited by H. Liebowitz), **2,** 591–619. Academic Press, New York.

Griffith, A. A. (1921). The phenomenon of rupture and flow in solids. *Philosophical Trans. R. Soc., London*, **A221,** 163–198.

Herrmann, H. J. and Roux, S. (Eds) (1990). *Statistical Models for the Fracture of Disordered Media*. North-Holland, Amsterdam.

Jayatilaka, A. S. (1979). *Fracture of Engineering Brittle Materials*. Applied Science, London.

Mandelbrot, B. B. (1982). *The Fractal Geometry of Nature*. W. H. Freeman and Company, New York.

Mandelbrot, B. B., Passoja, D. E. and Paullay, A. J. (1984). Fractal character of fracture surfaces of metals. *Nature* **308,** 721–722.

RILEM Technical Committee 50 (1985). Determination of the fracture energy of mortar and concrete by means of three-point bend tests on notched beams. Draft Recommendation, *Mater. Struct.* **18,** 287–290.

Saouma, V. E., Barton, C. C. and Gamaleldin, N. A. (1990). Fractal characterization of fracture surfaces in concrete. *Engng Fract. Mech.* **35,** 47–53.

Weibull, W. (1939). *A Statistical Theory for the Strength of Materials*. Swedish Royal Institute for Engineering Research, Stockholm.

Wilson, K. G. (1971). Renormalization group and critical phenomena. *Phys. Rev.* **B4,** 3174–3205.

Wilson, K. G. (1979). Problems in physics with many scales of length. *Scient. Am.* (Italian edition) **23,** 140–157.